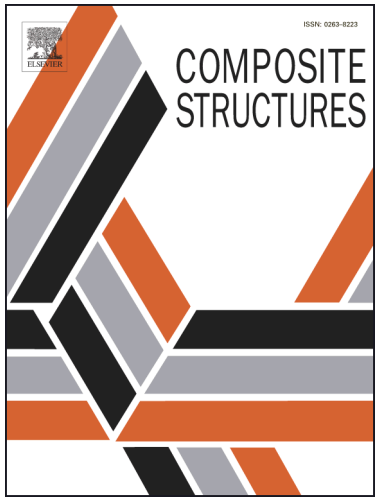

Bond strength model for externally bonded FRP-to-timber interface

Abbas Vahedian, Rijun Shrestha, Keith Crews

PII: S0263-8223(17)33410-4
DOI: https://doi.org/10.1016/j.compstruct.2018.05.152
Reference: COST 9791

To appear in: *Composite Structures*

Received Date: 17 October 2017
Revised Date: 5 May 2018
Accepted Date: 29 May 2018

Please cite this article as: Vahedian, A., Shrestha, R., Crews, K., Bond strength model for externally bonded FRP-to-timber interface, *Composite Structures* (2018), doi: https://doi.org/10.1016/j.compstruct.2018.05.152

Bond strength model for externally bonded FRP-to-timber interface

Abbas Vahedian[1], Rijun Shrestha, Keith Crews

Abbas Vahedian, School of Civil and Environmental Engineering, University of Technology, Sydney, Australia. abbas.vahedian@student.uts.edu.au

Dr Rijun Shrestha, School of Civil and Environmental Engineering, University of Technology, Sydney, Australia. Rijun.Shrestha-1@uts.edu.au

Prof Keith Crews, School of Civil and Environmental Engineering, University of Technology, Sydney, Australia. Keith.Crews@uts.edu.au

ABSTRACT

Despite the large number of studies on externally bonded elements using FRP composites, there is a significant knowledge gap to gain a comprehensive understanding of potential parameters such as bond width, bond length, material properties and geometries that influence bond strength. Behaviour of FRP bonded to concrete has been well investigated and there are a number of experimental and theoretical studies in this area; however, limited attempts have been made to investigate the bond behaviour of the FRP to timber interface. This paper reports an investigation on the behaviour of FRP externally bonded to timber. A novel theoretical model has been developed through stepwise regression analysis of 136 single shear FRP-to-timber joints. This has led to establishing a new predictive model for determination of the bond strength for FRP-to-timber joints. Results of this stepwise regression analysis are then assessed with results of experimental tests, and satisfactory comparisons have been achieved between ultimate applied loads and the predicted loads. Finally, a significant improvement in prediction of

[1] Corresponding author. Address: Faculty of Engineering and Information Technology, School of Civil and Environmental Engineering, the University of Technology, Sydney (UTS), Sydney 2007, NSW, Australia. Tel.: +61 4 5111 8680.

bond behaviour has been achieved when results of the proposed analytical model compared with the existing models from the literature, signifying the capability of the new models.

KEYWORDS: Bond strength, FRP, Timber, Pull-out test, Strain distribution profile

1 Introduction

There are large numbers of timber structures worldwide that have reached the end of their design service life. Moreover, ageing, inappropriate maintenance, surface degradation due to insect and fungal attack, environmental action, and increased service loads have caused many structures to gradually deteriorate and result in significant reduction in load capacity and subsequent safety. Consequently, either entire structures or key components now require strengthening, rehabilitation or replacement [1-3]. Recent [4-6] studies and applications have demonstrated that Fibre Reinforced Polymer (FRP) has become a mainstream technology for the strengthening of ageing and deteriorated structures.

FRPs are light, highly resistant to corrosion, cost effective and have superior strength and stiffness properties, whilst their specific strengths are capable of remaining high at elevated temperatures [4, 7]. FRP composite materials are able to carry high loads safely and increase the stability of structures and in some cases, are the only reasonable and applicable materials that can be used for retrofitting, particularly in places where it is impossible to gain access for heavy machinery [8]. These materials have a major role both in the field of strengthening and retrofitting of existing structures and in the new structural design [9]. External bonding of FRP composites has emerged as an innovative and widespread method for strengthening and retrofitting of infrastructure over the last three decades [5, 9, 10]. Although FRPs have a number of advantageous properties such as high elastic modulus, high fatigue performance, [9-11], they still have some important limitations.

One of the most common problems associated with the use the externally bonded FRP sheets is the premature failure due to debonding, which limits the full utilisation of the material strength of the FRP [12, 13]. Debonding can be defined as the single most important failure mechanism of retrofitted beams [14] that occurs at much lower FRP strains than its ultimate strain. Debonding directly impacts the total integrity of the structure, with the subsequent outcome that the ultimate capacity and desirable ductility of the structure may not be achieved.

A number of studies have been carried out experimentally [15-18] and theoretically [19, 20] to address the behaviour of FRP bonded to concrete substrate, masonry structures and more recently in structural glass beams [21, 22]. However, performance of FRP composite bonded externally to timber, considering debonding and other failure modes, has not been fully investigated and to date, limited attempts have been made to investigate the behaviour of FRP-to-timber joints. This study presents results of 136 Carbon Fibre Reinforced Polymer (CFRP) to timber joint with different bond width, bond length and cross-sectional size. Two different types of timber, namely Laminated Veneer Lumber (LVL) made out of softwood and kiln dried hardwood sawn timber, are utilised in this study. Factors affecting bond strength of FRP-to-timber joint have been investigated and subsequently, a proper constitutive model is introduced to accurately predict the ultimate strength of FRP-to-timber interface. Results of the proposed bond strength model are then assessed with results of pull-out tests and satisfactory comparisons are achieved. Finally, the predicted bond strength results have been then assessed by undertaking a comparative analysis with an existing model from the literature.

2 Experimental program

2.1 Detail of test setup and instrumentation

The experimental program in this study involved testing of 136 modified single shear CFRP-to-timber bonded interface as summarised in Table 1. Two different types of timber were used, namely Laminated Veneer Lumber (LVL) (using softwood species) and hardwood sawn timber. The LVL samples were of 320 or 370 mm length with a 110 mm x 65 mm cross section, and the overall dimension of hardwood samples was 320 mm long x 110 mm wide x 35 mm deep. One and two plies of unidirectional wet lay-up CFRP (MBRACE^{TM}) with the nominal thickness of 0.117mm were externally bonded with an epoxy base (Sikadur®-330) to the timber. In the LVL series, three different bond widths - 35 mm, 45 mm, and 55 mm, with five different bond lengths - 50 mm, 100 mm, 150 mm, 200 mm and 250 mm, were fabricated and tested. The hardwood samples included bond width of 45mm and bond lengths of 50 mm, 100 mm, 150 mm and 200 mm only. In all specimens, a 20 mm unbonded zone was provided at the loaded end to minimise wedge failure in the timber prism.

Strain gauges were attached to the CFRP surface to measure the strain variation along the length of the FRP and also to qualitatively monitor the bond behaviour. Strain gauges of 5 mm gauge length with 120.3 ±0.5 Ω resistance were bonded to the CFRP surface for each sample. One strain gauge was placed at the unbonded zone of the CFRP surface, and other strain gauges were distributed on the centre-line of FRP along the bond length as summarised in Table 2. Due to different bond length, the number of strain gauges varied between three to eight for the tested specimens.

Table 1, Detail of the tested specimens

Timber type	Identification of specimen	FRP Thickness (mm)	Bond Length (mm)	Bond Width (mm)	Number of specimens
Laminated Veneer Lumber	LVL 50-35-01		50	35	5
	LVL 100-35-01		100	35	5
	LVL 150-35-01		150	35	5
	LVL 200-35-01	1 x 0.117	200	35	5
	LVL 50-35-02		50	35	5
	LVL 100-35-02		100	35	5
	LVL 150-35-02		150	35	5
	LVL 200-35-02	2 x 0.117	200	35	5
	LVL 50-45-01		50	45	5
	LVL 100-45-01		100	45	5
	LVL 150-45-01		150	45	5
	LVL 200-45-01	1 x 0.117	200	45	5
	LVL 150-45-02	2 x 0.117	150	45	5
Hardwood	H 50-45-01		50	45	5
	H 100-45-01		100	45	5
	H 150-45-01		150	45	5
	H 200-45-01	1 x 0.117	200	45	5
	H 50-45-02		50	45	5
	H 100-45-02		100	45	5
	H 150-45-02		150	45	5
	H 200-45-02	2 x 0.117	200	45	5
Laminated Veneer Lumber	LVL 50-55-01		50	55	5
	LVL 100-55-01		100	55	5
	LVL 150-55-01		150	55	5
	LVL 200-55-01		200	55	5
	LVL 250-55-01	1 x 0.117	250	55	3
	LVL 150-55-02	2 x 0.117	150	55	5
	LVL 250-55-02	2 x 0.117	250	55	3

As shown in Figure 1, a modified single shear test setup was adopted to monitor bond behaviour and bond-slip relationships accurately. The bond-slip responses proposed by other researchers vary between a number of experimental studies presented in the literature. One reason for scattered results in the literature may be attributed to the test setup due to unexpected out of plane movements since the interface is under both shear and flexural stresses simultaneously. Besides, timber block may not be cut perfectly, so that these blocks cannot be tightly fitted and held in the frame. Therefore, some out-of-

plane movement of timber block can be expected. In this research, the timber block was restrained in a steel rig and load is applied to the free end of the FRP. The slip between timber and CFRP was also measured by a LVDT mounted on the surface of the timber block. It is important to note that in previous test setups [23], two or more LVDTs had been used for measuring the bond slip between timber and FRP; however, the slip was finally derived using the strain gauge profiles, since it was believed that the data collected from LVDTs are not reliable due to timber out-of-plane movement. Therefore, one of the key advantages of the present test setup when compared with previous test setups, is that when the timber block experiences any unexpected out of plane movements, both the timber and the LVDT's simultaneously have the same displacement. Moreover, at least one LVDT is omitted from the test, and the slip of interface can be measured with higher precision using only one LVDT placed at the loaded end. Figure 1 schematically shows the details of the specimens.

During preparation of the test specimens, the timber surface was sanded with 300 and 400 grit sandpaper to remove all contaminants and weak surface layers that can interfere with adhesion, and to develop a surface roughness. The timber surface was then wiped clean with acetone and air blasting. In addition, the surface of CFRP sheets was prepared as per ASTM-D2093-03 [24] and BSI [25] to remove all impurities and potential contaminants such as mould release agents, lubricants, or fingerprints as a result of the production process.

For each of the bond length, five specimens were tested, except for samples with 250 mm bond length where three specimens were tested. A preliminary set of tests was also

conducted with the intention to check the test rig set up and to evaluate the influence of potential parameters such as bond width, bond length, bond thickness, material properties and geometries on the bond strength. Accordingly, decisions were made as to the factors that were to be considered for further detailed investigation. All specimens were fabricated and epoxy was allowed to cure in the laboratory environment with 20°C to 22°C temperature and 60% to 70% relative humidity for at least 10 days. The pull-out tests were performed using a universal testing machine which had a capacity of 500kN. The maximum load range of 30 kN was applied based on predicted load capacity of sample tests as well as results of preliminary test samples which were in the range of 17-20kN. During pull-out tests, an initial 2 kN was applied and unloaded for all specimens and then the load was applied at the rate of 0.3 mm/min as per ISO 6238 [26] and ASTM D905-03 [27].

Table 2, Position of the strain gauges along the bonded length

	Distance of the strain gauges from the loaded end (mm)						
Bond length	SG2	SG3	SG4	SG5	SG6	SG7	SG8
50	15	40					
100	15	50	85				
150	15	50	85	120			
200	15	50	85	120	155	190	
250	15	50	85	120	155	190	225

[Insert Figure 1 here]

2.2 Material properties

The timber pieces used in this study were selected to be as free as possible from knots, pitch pockets and other natural growth features. The specimens used for material tests on timber were cut from the same timber members used to make the joint tests. A total of 28 timber samples (14 LVL and 14 hardwoods) were fabricated and tested in accordance with BS EN 408:2010 [28] to determine the mechanical properties of the timber prism. Tensile strength and elastic modulus of CFRP was determined based on tensile tests on six CFRP coupons following the ASTM D3039/D3039M Standard [29]. The epoxy adhesive was not tested; however, as per manufacture's product data sheet [30], the values of elastic modulus and tensile strength of Sikadur®-330 were 4.5GPa and 30MPa, respectively, and these values are used in the analytical phase of this study. The material test results are tabulated in Table 3.

Table 3, Material Properties of timber, FRP and adhesive

Material	Tensile		Compressive		Poisson ratio % (CoV)
	Tensile Strength MPa (CoV)	Modulus of Elasticity, GPa (CoV)	Compressive Strength MPa (CoV)	Modulus of Elasticity, GPa (CoV)	
Hardwood	67.53 (8.71)	19.75 (8.58)	64.93 (4.45)	19.70 (24.13)	0.36 (24.66)
LVL	44.31 (15.61)	16.18 (5.06)	56.26 (1.79)	17.68 (16.96)	0.30 (27.04)
FRP	2497 (6.45)	228.89 (10.22)	--	--	--
Sikadur®-330	30	4.5	--	--	--

CoV: co-efficient of variation

3 Factors affecting bond strength

The bond mechanism between timber and FRP is relatively complex and is influenced by a number of variables. Failure of a fibre reinforced polymer timber beam can take place in

several ways, including but not limited to substrate failure (timber separation), FRP delamination, FRP/adhesive separation, FRP rupture, cohesion failure (adhesive de-cohesion), adhesive failure, and substrate-to-adhesive interfacial failure. More than one of these modes may be observed in an actual failure. When debonding occurs, the stress shifts over a partial active area leading to local shear stress concentrations. Discontinuity near the ends of FRP is another reason of stress concentration [11]. Among the mentioned failure modes, adhesive failure occurs rarely due to its strong characteristic behaviour [31]; however, debonding between adhesive and adherent is often the critical failure mode since it has a significant influence on the performance of strengthened structures [14, 32].

Regardless of the effect of environmental conditions, surface treatment and moisture content, the bond strength depends significantly on the strength of the substrate material. Existing experimental investigations have suggested that the main failure mode associated to the externally bonded FRP joints is substrate failure under shear. Crews and Smith [33] reported that timber failure has been the main failure mode that occurred in their tests, indicating that the bond behaviour may be controlled by the properties of timber rather than that of the adhesive. Yao [32] also stated that substrate failure most often take place in pull-out tests under shear, occurring generally at a few millimetres from the adhesive layer. Therefore, it can be concluded that the substrate properties directly impact the bond strength.

Adhesive stiffness and adhesive strength are also reported amongst factors that impact the bond strength [34]; however, results of 86 single shear tests conducted by Wan [35]

stated that the properties of the adhesives used had not noticeably influenced the bond strength. A number of studies have also been carried out considering the behaviour of bond [14, 36-39] and their results show that the bond strength is highly dependent on the geometry of the bond and also varies with the FRP width and thickness, and the specimen alignment [14, 32]. Furthermore, it has also been observed that boundary conditions [14] and FRP to substrate width ratio [31] significantly impact on the bond strength. Another important parameter that significantly impacts on the bond strength is the bond length; however, effective bond length must always be taken into consideration. Many experimental studies [6, 14, 32, 36, 40] and fracture mechanics analyses [41, 42] have confirmed that there is no benefit in extending the bond length beyond the effective bond length where there is no increase in the bond strength. As mentioned above, there is a significant knowledge gap to gain a comprehensive understanding of parameters that influence the bond strength, particularly when FRP is bonded to timber. Therefore, a sound understanding of the behaviour of FRP-to-timber interface needs to be developed.

4 Existing bond strength and shear strength models

As noted previously, timber failure has been reported as the main failure mode in the study conducted by Crews and Smith [33], indicating that the bond behaviour may be controlled by the properties of timber rather than that of the adhesive. Wan [23] has conducted a more extensive study on FRP-to-timber interface in which results of 86 single shear tests are reported and correspondingly developed a bond strength model and bond stress-slip model for FRP-to-timber bond as follow:

$$P_u = 0.012\gamma_t\gamma_e b_f L_e^{0.28}\sqrt{E_f t_f} \quad (1)$$

$$\tau_{(x)} = \frac{dJ}{dx} = A^2 BC_N e^{-Bs}(1 - e^{-Bs}) \quad (2)$$

In Eq. (1), γ_t and γ_e were referred to timber sides and adhesive type, respectively. b_f, L_e and $E_f.t_f$ were referred to bond with, effective bond length and stiffness of FRP, respectively. In Eq. (2), *A* and *B* were experimental parameters, *s* was corresponding slip at specific location and C_n was referred to elastic stiffness. More explanation of these equations and parameters can be found in the study conducted by Wan [23].

The bond stress model proposed by Wan [23], Eq. (2), has been derived based on the theoretical proposals of Qiao and Chen [43] and Dai et al. [44] where concrete had been used as a substrate. In addition, the mechanical properties of timber was not considered in Eq. (1) because Wan [23] believed that softwood, hardwood and glulam used in the research were not significantly different from one another. As such, the importance of timber properties that have a major factor influencing the failure of the interface reported by others [33, 45] has been ignored in Wan's [23] model. Furthermore, in the Wan [23] study, the expression of the effective bond length was calculated using the model derived by Chen and Teng [31]. It is worth emphasising that Chen and Teng's model [31] was derived based on results of FRP-to-concrete interface. It is notable that there are some fundamental differences between the failure mechanism in timber and concrete when bonded with FRP. Concrete is weak in tension; whilst timber is often stronger in tension. Debonding initiates when the tensile stress at the interface exceeds the bond strength. Therefore, the models which work for FRP-to-concrete bond may not work for FRP-to-timber bond due to these differences. As a result, the bond strength model proposed by Wan [23] did not fit very well into the experimental results (Figure 2).

Consequently, for safe and economic design of FRP repair/strengthening of timber structures, further understanding of the bond is essential and thus, a new bond strength model for FRP-to-timber bonded interface is highly required to predict the ultimate load of the bond with better accuracy.

[Insert Figure 2 here]

5 Analysis of test results

A modelling analysis has been previously conducted by the authors [46] based on experimental results obtained from the literature (Wan [23]) for determining the key parameters affecting bond strength. It is important to note that the main focus in study performed by Wan [23] was on bond length and types of adhesive. However, other studies [23, 35] have concluded that the adhesives used does not noticeably influence the bond strength. In addition, in Wan's study [23], there were limited variations in parameters such as bond width, FRP-to-timber width ratio, tensile strength of timber, etc. The present experiments consist of all potential parameters and their impact on the bond strength as explained in the following sections.

5.1 Bond width series

Results from the tests with different bond widths, namely, 35 mm, 45 mm, and 55 mm, showed that the bond width significantly impacts on the bond strength; with the increase of the FRP plate width, the interfacial bond strength increases. This phenomenon may

lead to a decrease in the interfacial slip during the softening-debonded stage. In addition, results obtained from previous work conducted by the authors [6] showed that the maximum shear stress decreased with the increase of FRP-to-timber width ratio as shown in Figure 3. It is important to note that all bond characteristic and timber type in samples shown in Figure 3 are identical except for the bond width. This finding is in agreement with the previous studies when the FRP was bonded to concrete [11, 47, 48]. Figure 4 shows the local slip profiles along bonded length at various load levels for FRP with 35mm, 45mm and 55mm width; it can be seen that the local slip at the same level of applied load decreases with increasing FRP-to-timber width ratio. One reason can be highlighted that when FRP-to-timber width ratio is low, the force transfers from the FRP to timber leads to a non-uniform stress distribution across the width of timber leading to interfacial failure at lower load level. In addition, a smaller FRP width compared to the timber width may result in a higher stress in the bond at failure; directing stress from bonded area to the timber outside of the bonded zone. These findings are consistent with the previous studies conducted by [11, 38, 49].

[Insert Figure 3 here]

[Insert Figure 4 here]

5.2 Timber species series

Results of the experimental investigations showed that the main failure of the bond is attributed to timber failure as shown in Figure 5, occurring generally at a few millimetres from the adhesive layer. Whilst the tensile and compressive strength of the hardwood sawn timber were quite similar, LVL samples were stronger in compression, as shown in Table 3. FRP-timber joint specimens made from LVL exhibited a degree of ductile behaviour, failing gradually; while joints made from hardwood exhibited brittle behaviour, failing suddenly. The brittle failure of joints was more eminent when two layers of FRP were bonded to the timber. On the other hand, a higher ultimate load was recorded for specimens made from hardwood when compared with the joints made from LVL as shown in Figure 6. Higher tensile strength of the hardwood species therefore improved the bond strength. This finding is in agreement with observations made by Crews and Smith [33]. Therefore, it can be concluded that mechanical properties of the particular timbers been used need to be known for determining the bond strength when FRP is bonded to timber.

[Insert Figure 5 here]

[Insert Figure 6 here]

5.3 Bond length series

Many factors control the failure mode for an FRP strengthened beam. One of these factors is bond length and effective bond length must always be taken into consideration, since many experimental studies [14, 32, 36, 40] and fracture mechanics analyses [41, 42] have confirmed that there is no benefit in extending the bond length beyond that where there is no increase in the bond strength. Therefore, five different bond lengths (50mm, 100mm,150 mm, 200mm, and 250mm) were tested. The effective bond length of FRP-to-timber joints have been considered in the previous study conducted by authors [6] and a novel empirical model was derived (Eq 3).

$$L_e = \alpha \times \beta \times \ln(E_f t_f) \times (f_{ut})^{0.25} \quad (3)$$

$$\beta = \frac{1.25 + \frac{b_f}{b_t}}{2 \times (2.5 - \frac{b_f}{b_t})} \quad (4)$$

where E_f and t_f are the modulus of elasticity and thickness of FRP, respectively. f_{ut} is the ultimate tensile strength of timber block. The effect FRP to timber width ratio (β) (Eq. 4) was determined based on linear regression analysis using the test data of all specimens, where b_f and b_t are widths of FRP laminates and timber block, respectively.

Figure 7 shows the strain distribution profiles at various load levels along bonded length. It is important to mention that all bond characteristic and timber type in samples shown in Figure 7 are identical except bond length. Strain on point zero refers to the strain in the unbonded area. Three distinct profile trends can be identified from these strain

distribution diagrams based on the level of applied loads. In the first trend, the strain distribution exhibited a linear descending shape towards the end of the bond as the load was initially applied. This downward pattern represents that the stress transfer length has been constant. The second trend shows that the strain increased gradually between strain gauges 2 and 4 until crack initiated in the interface. Although all sample results are not shown here, it was observed that the maximum load associated with this strain distribution occurred approximately at 60% to 65% of the ultimate applied load, depending on bond geometries. This observation is more evident when the bond length was equal or longer than effective bond length as shown in Figure 7 (d) and Figure 9. However, for those samples where the bond length was not long enough debonding occurred at much lower FRP strains than its ultimate strain. Accordingly, the distance from loaded end to the point where the strain profile reaches zero defines the so-called initial transfer length. Once a crack is formed, the effective bond zone propagates from the loaded end toward the unloaded end and a further increase in strain distribution was observed until the applied loading P reached ultimate load P_u. In the third trend, Figure 7, there is a bilinear tendency in the strain distribution with a transition point occurring at the limit of the initial transfer area. In the current study, this transition point generally coincided with approximately 75% of the ultimate load, and in some other samples around 80% of the ultimate load was recorded. The bilinear trend in strain distribution is different from the theoretical relationship between the FRP sheet strain and the distance from the loaded end since it is expected to be uniform for completely homogeneous material. This phenomenon may be due to material heterogeneity or stress concentration in the FRP plate and timber at a meso-scale [11, 19]. It should be noticed that when the

bond length is long enough, the strain gauges near the far end of bond experience quite minimal strain values.

The average ultimate loads for the specimens represented in Figure 7 (a-d) are 5.27kN, 6.27kN, 7.66kN and 7.94kN, respectively. The ultimate load of specimens (c) and (d) are relatively similar; however, their values are approximately 1.5 times higher than the peak load obtained for specimens (a) and 1.26 times of the ultimate load obtained for specimens (b). One reason may be due insufficient bond length in specimens (a and b), since the bond length of specimens (a) and (b) are 50mm and 100mm, respectively, while the predicted effective bond length using Eq. (3) is 134mm. Therefore, premature debonding can be expected at lower FRP strains limiting the full utilisation of the bond. On the other hand, when the bond length is long enough, the strain gauges near the far end of bond experience quite minimal strain values as shown in Figure 7 (d). Nevertheless, debonding starts when the relative slip between FRP and timber exceeds the ultimate slip. At this point, the ultimate load that can be carried by the FRP plate is attained and simultaneously, the effective bond zone shifts towards the free end of the bond. Therefore, the ultimate load P_u remains almost constant. This condition signifies the concept of effective bond length that there is no benefit in extending the bond length beyond that where there is no increase in the bond strength.

In the present study, experimental tests results revealed that bond width, bond stiffness and timber strength are the key parameters that significantly affect the bond strength of FRP-to-timber interface. Figure 8 shows the effect of bond width (FRP-to-timber width ratio), bond length and type of timber on the bond strength. As can be seen, the bond

strength has significantly increased when the bond width and timber tensile strength increased. In addition, bond length directly has a major impact on the bond strength; however, bond strength cannot increase further once the bond length exceeds the effective bond length. Nevertheless, a longer bond length can improve the ductility of the interface [38].

[Insert Figure 7 here]

[Insert Figure 8 here]

[Insert Figure 9 here]

6 Proposed bond strength model

The average shear stress between two consecutive strain gauge positions and thus the shear stress distribution can be determined as follows [36]:

$$\tau_{i-j} = \frac{t_f \times E_f \times (\varepsilon_i - \varepsilon_j)}{\Delta l_{i-j}} \quad (5)$$

where ε_i and ε_j are two strain gauges at positions *i* and *j*, and Δl_{i-j} is the distance between these two gauges. E_f and t_f are elastic modulus and thickness of the laminate, respectively. Proceeding in this way for all gauge positions, results of stress distribution along the interface can be obtained. Stress distribution along the bonded length for two specimens are shown in Figure 10 as an example. Furthermore, Figure 11 illustrates the evaluation of shear stress distribution along the bonded length as a function of the relative load. It can be seen that the shear stress in the region near the bearing end reaches a peak (P_{max}) and then begins to decrease abruptly, while simultaneously the shear stress in the adjacent region is beginning to increase. It is important to be noted that, the decrease of the shear stress signifies failure in one region, while ascending of shear stress in the adjacent region illustrates that the load is being transferred there. Thus, the effective bond zone is being shifted inward along the bond length. This phenomenon was constantly observed such that the region of high stress transferred from one area to the adjacent area until the total failure of the bond occurred.

[Insert Figure 10 here]

[Insert Figure 11 here]

As emphasised in section 5, the ultimate bond strength has been mostly related to bond width, bond stiffness, timber strength and the bond length. Therefore, stepwise regression (SR) as a robust approach has been used for selecting the best combination of independent variables that best fits the dependent variable (the ultimate load (*Pu*) in the present study). When dealing with a large group of potential independent variables, stepwise regression can be employed to determine the most significant variables in predicting the dependent variable [50]. Stepwise regression is a robust approach for selecting the best subset of independent variables that provides efficient prediction of the dependent variable. In addition, such analysis significantly reduces computing complexity than is required for all possible regressions [51]. Stepwise regression is a combination of Forward and Backward selection. In Forward selection, the determination of the best subset models can be obtained either by trying out one independent variable into the regression model that produces the highest value of R-Squared if statistical significance of model is kept. Whilst, Backward selection includes all potential independent variables in the regression model and removing those that are least significant. Stepwise regression is a combination of these two methods, selecting variable(s) that has the highest effect on the residual sum of squares; and

conversely, removing the variable(s) that has the least significant on the residual sum of squares.

However, the verification of the capability of the model proposed by SR is not only to rely value of R-squared or the model's P-value (an indicator that describes whether or not a variable has statistically significant predictive capability in the presence of the other variable), but instead, assess the model against an "independent" data set that was not used to create the model [52]. Thus, a model can be built based on a sample of the dataset available (e.g., 70%) and then, assess the accuracy of the model using the remaining 30% dataset [53]. Accordingly, a database including 100 experimental results of the FRP-to-timber joint has been used to create the model (predict) and remaining 36 sets of data have been used to test the measurement accuracy of SR model. Statistical Analysis Software (SAS®) was used for the stepwise regression analysis. SAS®, which permits choosing the stepwise variable selection option by providing the opportunity to specify the method as "Forward" or "Backward". In the present study, a fully stepwise analysis has been selected (both Forward and Backward methods) allowing the software to perform a straight multiple regression using all the variables. The stepwise selection process has been performed using different possible combinations of independent variables including linear; polynomial; exponential model; reciprocal model and nonlinear multiple regression. A simple analytical formula but with a superior accuracy has been derived covering those critical variables that influence on the bond strength as follows:

$$P_u = \gamma_t . \sqrt{L_e . f_{ut} . E_f t_f . \left(\frac{b_f}{b_t}\right)^3} \qquad (6)$$

The units for the above equation are: Megapascals, Newtons, and millimetres, where, b_f, E_f and t_f are the FRP width, elastic modulus and thickness of FRP sheet, respectively. f_{ut} and b_t refer to the ultimate tensile strength and width of the timber prism, respectively. L_e is the effective bond length derived using Eq. (3). The latter parameter γ_t is related to the timber types, in which γ_t is equal to 0.1 and 0.08 for LVL and hardwood, respectively.

Figure 12 shows the evaluation of the stepwise regression model of FRP-to-timber bonded interface against experimental results. Results of the analytical solution (Eq. 6) presented in this paper have been compared with the existing model proposed by [23] (Eq. 1) to evaluate the capability of the proposed model and also to demonstrate the improvement of the current analytical model against previous model. As shown in Figure 2 and Figure 12, it is interesting to note that the coefficient of determination (R^2) of the stepwise regression analysis signifies that the SR model (R^2=0.89) is even more enhanced when compared with the model proposed by [23] (R^2=0.59) and is a more accurate predictor than the existing model.

[Insert Figure 12 here]

Apart from regression analysis, reliability of the derived model was also assessed based on the Integral Absolute Error (IAE, %). This index has been used by other

researchers [54, 55] to evaluate the performance of the fitted model. In Eq. (7), O_i and P_i are the observed and predicted values, respectively. The value of zero rarely occurs for IAE; however, having a regression model with a low value of IAE demonstrates that the derived model is reliable. For an acceptable regression equation, a range of 0 to 10% is suggested in the literature [56, 57]. The Integral Absolute Error of 0.9% was obtained using Eq. (7) for the proposed model against experimental results which is quite low and is in agreement with recommendations made in the literature [56, 57], emphasising the reliability of proposed model.

$$IAE = \sum \frac{\sqrt{(O_i - P_i)^2}}{\sum O_i} \times 100 \tag{7}$$

7 Discussion

Apart from ultimate bond strength, the bond stress also needs to be considered to evaluate the capability of the interface for both ultimate and serviceability limit state designs. As mentioned above, when the applied load increases, the shear stress in the region near the loaded end reaches up to the maximum value and then begins to decrease abruptly. The decrease of the shear stress signifies that debonding is formed in one region, while ascending of shear stress in the adjacent region illustrates that the load is being transferred there. In the majority of sample tests, it was observed that the debonding has initiated approximately at 60% to 65% of the ultimate applied load (as shown in Figure 7 (d) and Figure 9, Figure 11), depending on bond geometries. Therefore, the coefficient (γ_t) in Eq. (6) may be reduced by 60% to control the interface for both ultimate and serviceability limit state (without debonding).

The analytical model, Eq. (8), proposed in the recent study conducted by authors has been used for determining bond stress along the interface. In addition, the accuracy of the proposed analytical model has been compared with the model proposed by Wan et al. [35]. Figure 13 shows bond stress profiles at various load levels obtained from experimental tests, Wan's model [35] Eq. (2), and Eq. (8) of the present study.

$$\tau_{(x)} = \frac{6P}{b_f L_e^{\,2}}\left(1-\frac{x}{L_e}\right).x$$

$$\tau_{(\max)} = \frac{3P_u}{2b_f.L_e} \qquad (8)$$

Where $\tau_{(x)}$ is the bond stress, *P* is the applied load, and x = 0 corresponds to the free end and x = L represents the loaded end. The proposed analytical model predicts the nature of the stress profile at most load levels, particularly at or close to the ultimate load. Good correlation between the predicted maximum stress from the proposed model and experimental results has been obtained. Comparison of results with existing model [35] also shows that the proposed model is able to achieve much better correlation with the experimental results. Table 4 provides the configuration and results of the selected specimens as well as bond strength obtained from experimental tests and the current proposed bond strength model. Although all sample results are not presented in Table 4, the ratio of the predicted bond strength to the bond strength obtained from experimental results for all sample tests has an average value of 1.00 with the coefficient of variation of 8.5%. It can be seen that, SR model not only performs significantly better than the existing model, but also high correlation has been obtained when SR model has been compared against the experimental test as

shown in Figure 12. In addition, Table 4 shows the comparison of measured effective bond length using strain profile with the predicted effective bond length using Eq. (3) in the present study. As can be seen, superior correlation has been obtained for the proposed effective bond length model against the experimental results.

Table 4, Selected test results

Specimen Codes	Timber			FRP			Effective bond length			b_f/b_t	S_{max} (mm)	τ_{max} (MPa)	Pu (kN)		
	L_t (mm)	b_t (mm)	d_t (mm)	t_f (mm)	B_f (mm)	$E_f t_f$ (Gpa.mm)	L_f (mm)	(EXP. mm)	(Anal. mm)				(Exp.)	(Anal.)	(Anal. /Exp.)
LVL 50-35-01-2	320	110	65	0.117	35	27	50	50	134	0.32	0.305	1.69	4.92	4.37	0.89
LVL 100-35-01-1	320	110	65	0.117	35	27	100	100	134	0.32	0.412	2.20	6.35	6.18	0.97
LVL 150-35-01-2	320	110	65	0.117	35	27	150	129	134	0.32	0.920	3.42	7.27	7.57	1.04
LVL 200-35-01-4	320	110	65	0.117	35	27	200	136	134	0.32	0.884	4.67	8.75	8.74	1.00
LVL 50-45-01-3	320	110	65	0.117	45	27	50	50	148	0.41	0.202	1.36	6.09	6.37	1.05
LVL 100-45-01-1	320	110	65	0.117	45	27	100	100	148	0.41	0.640	3.30	9.07	9.01	0.99
LVL 150-45-01-3	320	110	65	0.117	45	27	150	146	148	0.41	0.725	2.62	10.15	11.04	1.09
LVL 200-45-01-3	320	110	65	0.117	45	27	200	182	148	0.41	1.760	3.30	11.13	12.75	1.14
LVL 50-55-01-1	320	110	65	0.117	55	27	50	50	163	0.50	0.334	2.63	8.05	8.61	1.07
LVL 100-55-01-2	320	110	65	0.117	55	27	100	100	163	0.50	0.655	3.47	12.50	12.18	0.97
LVL 150-55-01-1	320	110	65	0.117	55	27	150	169	163	0.50	0.736	2.98	14.48	14.92	1.03
LVL 200-55-01-3	320	110	65	0.117	55	27	200	180	163	0.50	1.296	4.37	15.74	17.22	1.09
LVL 250-55-01-1	370	110	65	0.117	55	27	250	190	163	0.50	1.227	1.52	15.32	19.26	1.26
LVL 50-35-02-1	320	110	65	0.234	35	54	50	50	143	0.32	0.186	3.04	7.00	6.18	0.88
LVL 100-35-02-3	320	110	65	0.234	35	54	100	100	143	0.32	0.548	5.59	8.45	8.74	1.04
LVL 150-35-02-2	320	110	65	0.234	35	54	150	140	143	0.32	0.845	4.85	10.99	10.71	0.97
LVL 200-35-02-4	320	110	65	0.234	35	54	200	149	143	0.32	0.749	3.71	12.32	12.37	1.00
LVL 150-45-02-3	320	110	65	0.234	45	54	150	151	158	0.41	0.818	3.91	16.75	15.61	0.93
LVL 150-55-02-1	320	110	65	0.234	55	54	150	180	174	0.50	0.553	3.76	16.72	16.88	1.01
LVL 250-55-02-3	370	110	65	0.234	55	54	250	194	174	0.50	0.966	5.56	20.40	21.79	1.07
H 50-45-01-3	320	110	35	0.117	45	27	50	50	164	0.41	0.340	2.86	5.92	6.29	1.06
H 100-45-01-1	320	110	35	0.117	45	27	100	100	164	0.41	0.595	3.35	8.83	8.90	1.01
H 150-45-01-4	320	110	35	0.117	45	27	150	157	164	0.41	0.879	3.88	9.91	10.90	1.10
H 200-45-01-4	320	110	35	0.117	45	27	200	191	164	0.41	1.210	2.01	12.03	12.59	1.05
H 50-45-02-2	320	110	35	0.234	45	54	50	50	175	0.41	0.192	4.56	9.16	8.90	0.97
H 100-45-02-1	320	110	35	0.234	45	54	100	100	175	0.41	0.602	5.67	11.56	12.59	1.09
H 150-45-02-3	320	110	35	0.234	45	54	150	170	175	0.41	0.877	7.24	16.13	15.42	0.96
H 200-45-02-4	320	110	35	0.234	45	54	200	185	175	0.41	0.963	5.21	16.05	17.80	1.11

[Insert Figure 13 here]

8 Conclusion

This paper presents the application of a stepwise regression analysis for determining the key parameters affecting bond strength when the FRP plates are externally attached to timber and evaluate their influence on the bond strength. The proposed stepwise regression model is based on 136 experimental results of FRP-to-timber single shear pull out tests.

A novel and simple predictive bond strength model with a higher accuracy for FRP-to-timber joints has been established covering all parameters affecting the interface. The proposed model is a function of bond stiffness, timber tensile strength, FRP to timber width ratio and bond length. A comparative analysis of the results of the experimental pull-out tests results and those predicted from the analytical model demonstrated the capability of the model in prediction of the ultimate load.

Results of the proposed model has been assessed by undertaking a comparative analysis with existing model from the literature to verify the capability of the new model. It is noted that the coefficient of determination (R^2) of the stepwise regression

analysis signifies that the SR model is even more enhanced and is a more accurate predictor than the existing bond strength model.

The scope of the present study is limited to results of experimental tests; however, the derived model is considered to be generally applicable to externally bonded FRP-to-timber joints. Additional research will be needed to further verify the proposed model for more general applications and also to address long-term response issues. This study is a part of an ongoing research project aiming to scrutinise all potential parameters affecting bond strength, particularly when FRP is bonded to timber. Due to the lack of studies available in the literature, the future research includes numerical investigation which is one of the most neglected fields of research especially in the area of FRP-to-timber interface.

Acknowledgement

The authors wish to acknowledge the support provided by Australian Government Research Training Program Scholarship. The support of Sika Australia Pty. Ltd., who supplied the materials for this study, is gratefully acknowledged.

References:

1. Shrestha, R., *Behaviour of RC beam-column connections retrofitted with FRP strips*, in *Faculty of Engineering and Information Technology*. 2009, University of Technology Sydney.
2. Borri, A. and M. Corradi, *Strengthening of timber beams with high strength steel cords.* Composites Part B: Engineering, 2011. **42**: p. 1480–1491.
3. Borri, A., M. Corradi, and A. Grazini, *A method for flexural reinforcement of old wood beams with CFRP materials.* Composites Part B: Engineering, 2005. **36**(2): p. 143-153.
4. Kabir, M.I., B. Samali, and R. Shrestha, *Fracture properties of CFRP–concrete bond subjected to three environmental conditions.* Journal of Composites for Construction, 2016. **20**(4): p. 04016010.
5. Kabir, M.I., R. Shrestha, and B. Samali, *Effects of applied environmental conditions on the pull-out strengths of CFRP-concrete bond.* Construction and Building Materials, 2016. **114**: p. 817-830.
6. Vahedian, A., R. Shrestha, and K. Crews, *Effective bond length and bond behaviour of FRP externally bonded to timber.* Construction and Building Materials, 2017. **151**: p. 742-754.
7. De la Rosa García, P., A.C. Escamilla, and M.N.G. García, *Bending reinforcement of timber beams with composite carbon fiber and basalt fiber materials.* Composites Part B: Engineering, 2013. **55**: p. 528-536.
8. Motavalli, M. and C. Czaderski, *FRP composites for retrofitting of existing civil structures in Europe: state-of-the-art review.* Proceedings of the American Composites Manufacturers Association 2007, 2007.
9. Juvandes, L. and R. Barbosa, *Bond Analysis of Timber Structures Strengthened with FRP Systems.* Strain, 2012. **48**(2): p. 124-135.
10. Valipour, H.R. and K. Crews, *Efficient finite element modelling of timber beams strengthened with bonded fibre reinforced polymers.* Construction and Building Materials, 2011. **25**(8): p. 3291-3300.
11. Xu, T., Z. He, C. Tang, W. Zhu, and P. Ranjith, *Finite element analysis of width effect in interface debonding of FRP plate bonded to concrete.* Finite Elements in Analysis and Design, 2015. **93**: p. 30-41.
12. Khelifa, M. and A. Celzard, *Numerical analysis of flexural strengthening of timber beams reinforced with CFRP strips.* Composite Structures, 2014. **111**: p. 393-400.
13. Wu, Z. and S. Hemdan. *Debonding in FRP Strengthened Flexural Members with Different Shear-Span Ratios*. in *Proceeding of the 7th International Symposium on Fiber Reinforced Composite Reinforcement for Concrete Structures*. 2005. Michigan, USA.
14. Coronado, C., *Characterization, modeling and size effect of concrete-epoxy interfaces*, in *Department of Civil and Environmental Engineering*. 2006, The Pennsylvania State University.
15. Cao, S., J. Chen, J. Pan, and N. Sun, *ESPI measurement of bond-slip relationships of FRP-concrete interface.* Journal of Composites for Construction, 2007. **11**(2): p. 149-160.
16. Mazzotti, C., M. Savoia, and B. Ferracuti, *An experimental study on delamination of FRP plates bonded to concrete.* Construction and Building Materials, 2008. **22**(7): p. 1409-1421.
17. Nakaba, K., T. Kanakubo, T. Furuta, and H. Yoshizawa, *Bond behavior between fiber-reinforced polymer laminates and concrete.* ACI Structural Journal, 2001. **98**(3).
18. Aram, M.R., C. Czaderski, and M. Motavalli, *Debonding failure modes of flexural FRP-strengthened RC beams.* Composites part B: engineering, 2008. **39**(5): p. 826-841.

19. Dai, J., T. Ueda, and Y. Sato, *Unified analytical approaches for determining shear bond characteristics of FRP-concrete interfaces through pullout tests.* Journal of Advanced Concrete Technology, 2006. **4**(1): p. 133-145.
20. Ferracuti, B., M. Savoia, and C. Mazzotti, *Interface law for FRP–concrete delamination.* Composite structures, 2007. **80**(4): p. 523-531.
21. Bedon, C. and C. Louter, *Numerical analysis of glass-FRP post-tensioned beams–review and assessment.* Composite Structures, 2017. **177**: p. 129-140.
22. Bedon, C. and C. Louter, *Numerical investigation on structural glass beams with GFRP-embedded rods, including effects of pre-stress.* Composite Structures, 2018. **184**: p. 650-661.
23. Wan, J., *An investigation of FRP-to-timber bonded interfaces*, in *Civil Engineering*. 2014, The University of Hong Kong Pokfulam, Hong Kong.
24. ASTM-D2093-03, *Standard Practice for Preparation of Surfaces of Plastics Prior to Adhesive Bonding.*, in *American Society for Testing and Materials*. 2003, West Conshohocken, PA: USA.
25. BSI, *Structural Adhesives – Guidelines for the Surface Preparation of Plastics*, in *BS EN 1840*. 1995, British Standards Institution: London, UK,.
26. ISO6238, *Adhesives -- Wood-to-wood adhesive bonds -- Determination of shear strength by compressive loading*, in *the International Organization for Standardisation*. 2001.
27. ASTM-D905-03, *Standard test method for strength properties of adhesive bonds in shear by compression loading*, in *American Society for Testing and Materials*. 2003, West Conshohocken, PA: USA,.
28. BS_EN_408, *Timber structures - structural timber and glued laminated timber - determination of some physical and mechanical properties*, in *BS EN 408:2010*. 2010, British Standards Institution: London, UK,.
29. ASTM-D3039/D3039M, *Standard test method for tensile properties of polymer matrix composite materials*, in *American Society for Testing and Materials*. 2014, West Conshohocken, PA: USA,.
30. Sikadur®-330. *2-part epoxy impregnation resin, Product Data Sheet*. 2015.
31. Chen, J. and J. Teng, *Anchorage strength models for FRP and steel plates bonded to concrete.* Journal of Structural Engineering, 2001. **127**(7): p. 784-791.
32. Yao, J., J. Teng, and J. Chen, *Experimental study on FRP-to-concrete bonded joints.* Composites Part B: Engineering, 2005. **36**(2): p. 99-113.
33. Crews, K. and S.T. Smith. *Tests on FRP-strengthened timber joints*. in *Proceedings, 3rd International Conference on FRP Composites in Civil Engineering, CICE 2006*. 2006.
34. Vallée, T., T. Tannert, J. Murcia-Delso, and D.J. Quinn, *Influence of stress-reduction methods on the strength of adhesively bonded joints composed of orthotropic brittle adherends.* International Journal of Adhesion and Adhesives, 2010. **30**(7): p. 583-594.
35. Wan, J., S.T. Smith, P. Qiao, and F. Chen, *Experimental Investigation on FRP-to-Timber Bonded Interfaces.* Journal of Composites for Construction, 2013.
36. Bizindavyi, L. and K. Neale, *Transfer lengths and bond strengths for composites bonded to concrete.* Journal of composites for construction, 1999. **3**(4): p. 153-160.
37. Gómez, S. and D. Svecova, *Behavior of split timber stringers reinforced with external GFRP sheets.* Journal of Composites for Construction, 2008. **12**(2): p. 202-211.
38. Hollaway, L.C. and J.-G. Teng, *Strengthening and rehabilitation of civil infrastructures using fibre-reinforced polymer (FRP) composites*. 2008, North America by CRC Press: Elsevier Reference Monographs.
39. McSweeney, B., *FRP-concrete bond behavior: A parametric study through pull-off testing*, in *Department of Civil and Environmental Engineering*. 2005, Pennsylvania State University.

40. Franco, A. and G. Royer Carfagni, *Effective bond length of FRP stiffeners.* International Journal of Non-Linear Mechanics, 2014. **60**: p. 46-57.
41. Yuan, H. and Z.S. Wu. *Interfacial fracture theory in structures strengthened with composite of continuous fiber*. in *Proceedings of symposium of China and Japan: Science and technology of 21st century*. 1999.
42. Yuan, H., Z.S. Wu, and H. Yoshizawa, *Theoretical solutions on interfacial stress transfer of externally bonded steel/composite laminates.* J. Struct. Mech. and Earthquake Engrg.,, 2001(675): p. 27-39.
43. Qiao, P. and F. Chen, *Interface crack between two interface deformable piezoelectric layers.* International Journal of Fracture, 2009. **156**(2): p. 185-201.
44. Dai, J., T. Ueda, and Y. Sato, *Development of the nonlinear bond stress–slip model of fiber reinforced plastics sheet–concrete interfaces with a simple method.* Journal of Composites for Construction, 2005. **9**(1): p. 52-62.
45. Kim, Y.J. and K.A. Harries, *Modeling of timber beams strengthened with various CFRP composites.* Engineering Structures, 2010. **32**(10): p. 3225-3234.
46. Vahedian, A., R. Shrestha, and K. Crews, *Modelling the bond slip behaviour of FRP externally bonded to timber*, in *The World Conference on Timber Engineering (WCTE 2016)*. 2016: Vienna, Austria.
47. Chen, J. and W. Pan, *Three dimensional stress distribution in FRP-to-concrete bond test specimens.* Construction and Building Materials, 2006. **20**(1): p. 46-58.
48. Ye, F. and J. Yao, *A 3D Finite Element Study on The Effect of FRP Plate Width on Interfacial Stress between FRP and Concrete [J].* Bulletin of Science and Technology, 2008. **24**(6): p. 853-859.
49. Vahedian, A., R. Shrestha, and K. Crews, *Analysis of externally bonded Carbon Fibre Reinforced Polymers sheet to timber interface.* Composite Structures, 2018. **191**.
50. Cevik, A., M.T. Göğüş, İ.H. Güzelbey, and H. Filiz, *Soft computing based formulation for strength enhancement of CFRP confined concrete cylinders.* Advances in Engineering Software, 2010. **41**(4): p. 527-536.
51. Campbell, M.J., *Statistics at square two: understanding modern statistical applications in medicine*. 2006: BMJ Books/Blackwell.
52. Mark, J. and M.A. Goldberg, *Multiple regression analysis and mass assessment: A review of the issues.* Appraisal Journal, 1988. **56**(1).
53. Myers, J.H. and E.W. Forgy, *The development of numerical credit evaluation systems.* Journal of the American Statistical Association, 1963. **58**(303): p. 799-806.
54. Shen, D., H. Shi, Y. Ji, and F. Yin, *Strain rate effect on effective bond length of basalt FRP sheet bonded to concrete.* Construction and Building Materials, 2015. **82**: p. 206-218.
55. Wu, Y.-F. and Y.-W. Zhou, *Unified strength model based on Hoek-Brown failure criterion for circular and square concrete columns confined by FRP.* Journal of Composites for Construction, 2010. **14**(2): p. 175-184.
56. Arıoglu, N., Z.C. Girgin, and E. Arıoglu, *Evaluation of ratio between splitting tensile strength and compressive strength for concretes up to 120 MPa and its application in strength criterion.* ACI Materials Journal, 2006. **103**(1): p. 18-24.
57. Girgin, Z.C., N. Arioglu, and E. Arioglu, *Evaluation of strength criteria for very-high-strength concretes under triaxial compression.* ACI structural journal, 2007. **104**(3): p. 278.

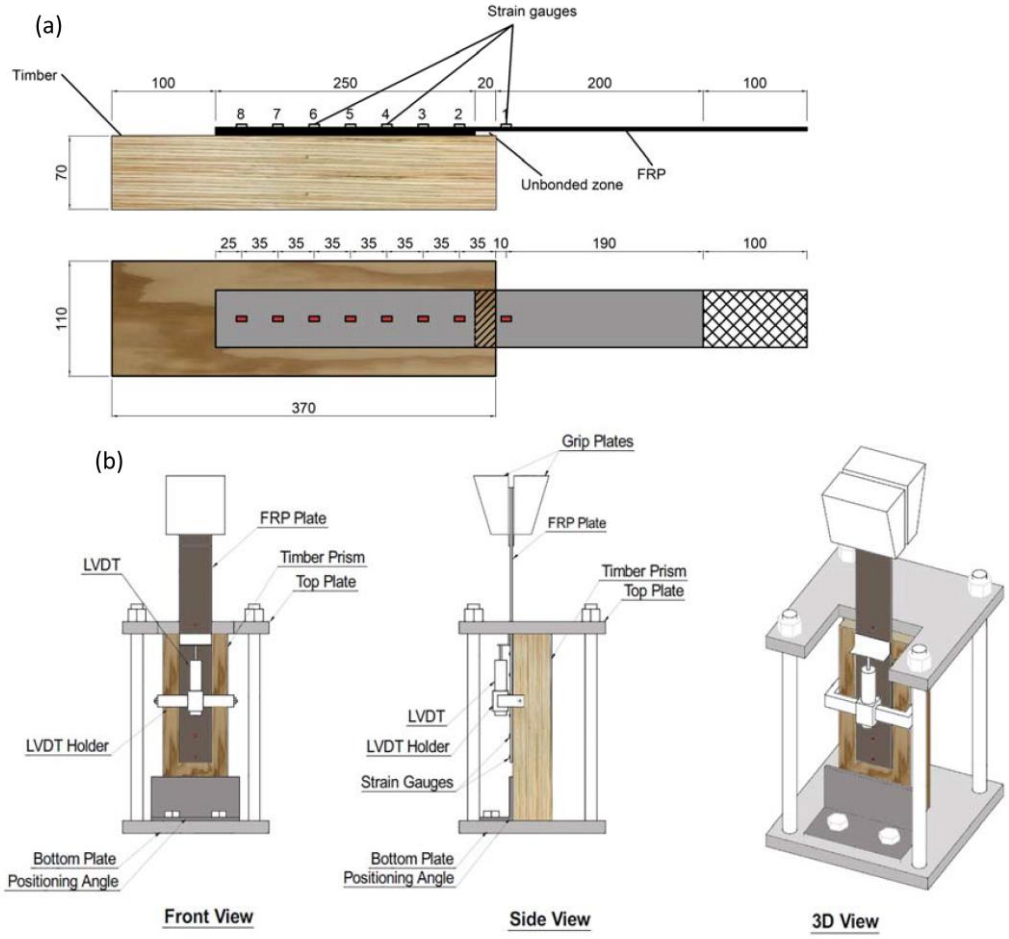

Figure 1, Modified test setup; application of the strain gauges on the bonded joint (a), schematic view (b); all dimensions are in millimetres

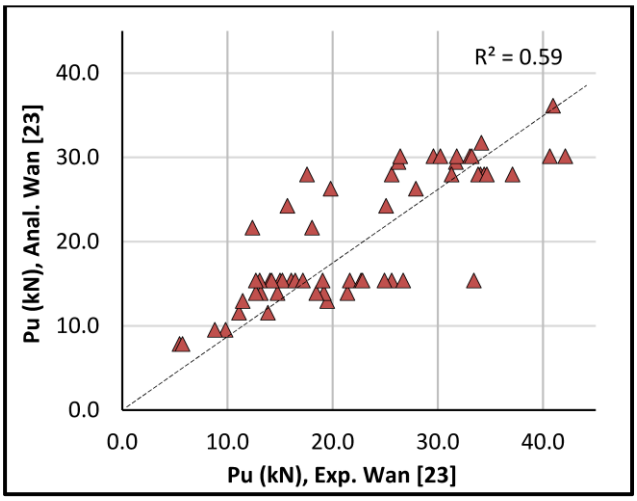

Figure 2, Comparison of bond strength; experimental and analytical model proposed by Wan [23]

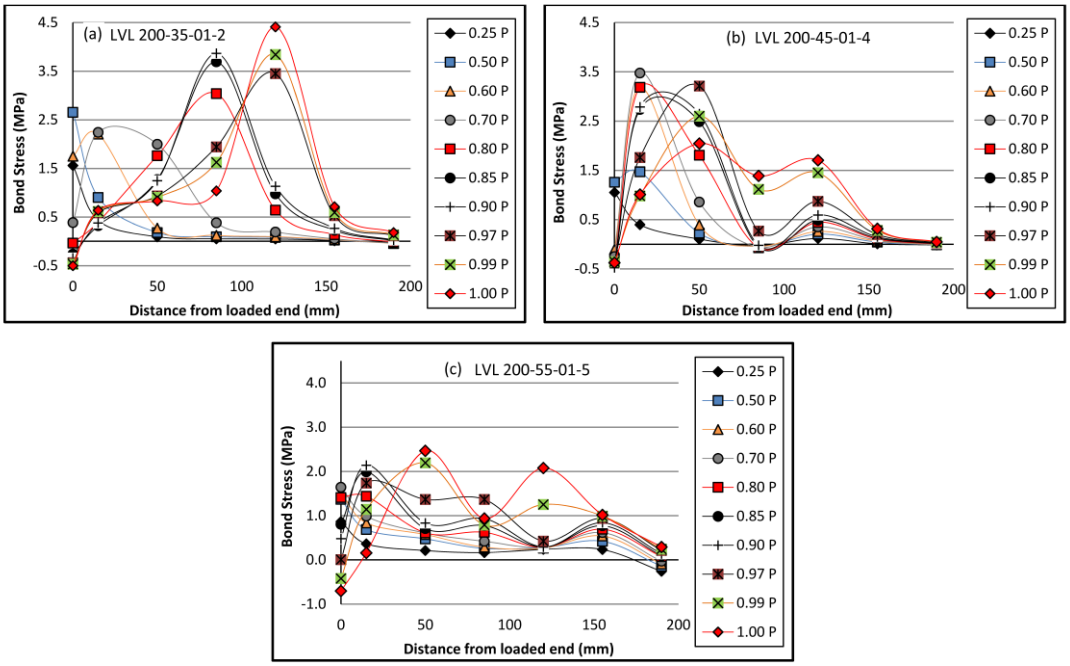

Figure 3, Relationship between bond stress and FRP-to-timber width ratio; (a) 32%, (b) 41% and (c) 50%

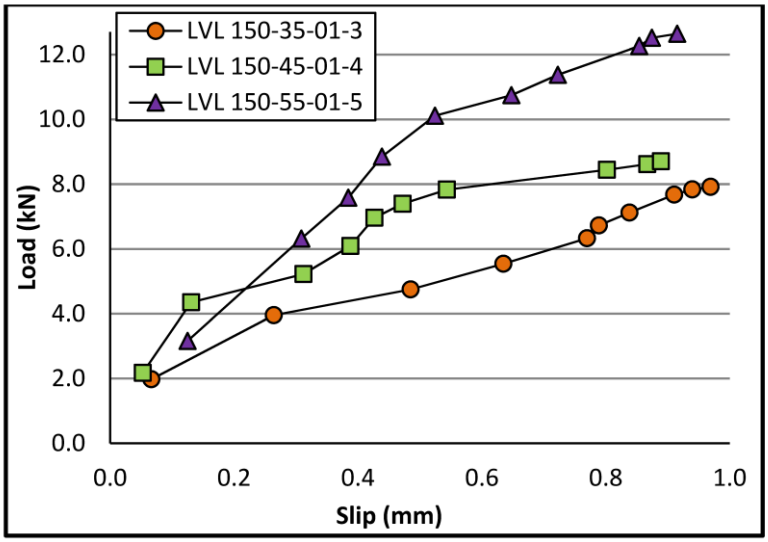

Figure 4, Relationship between local slip and bond width

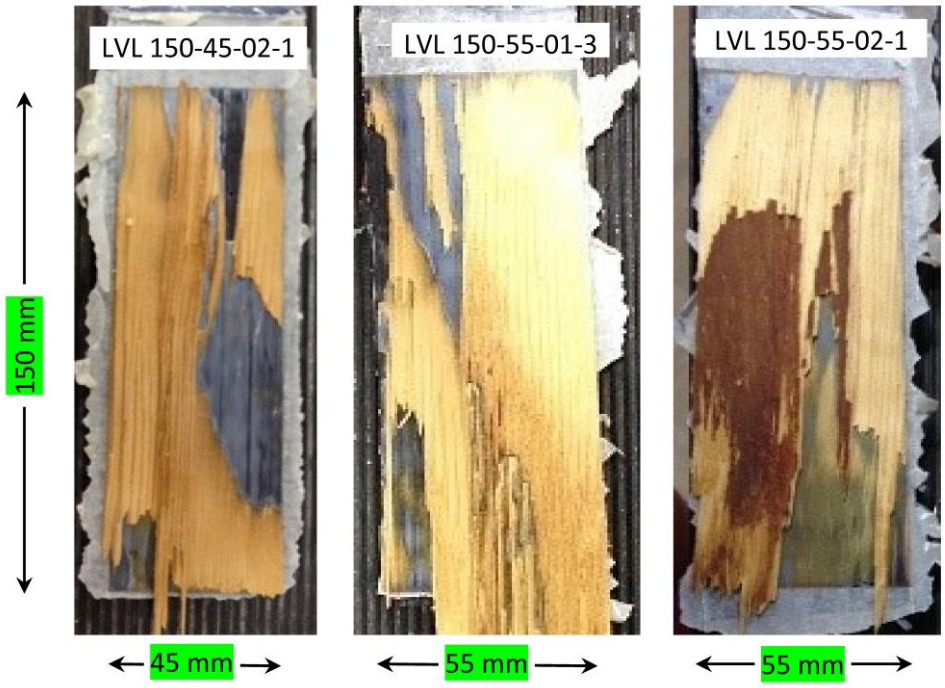

Figure 5, The main failure mode, timber attached to the FRP

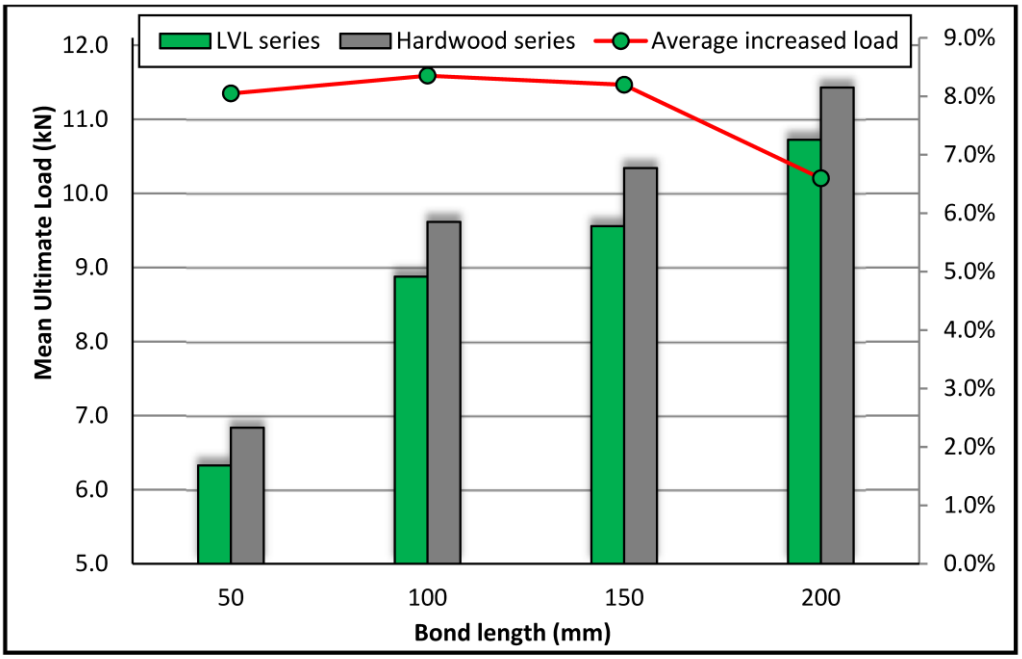

Figure 6, Relationship between ultimate applied local and timber type

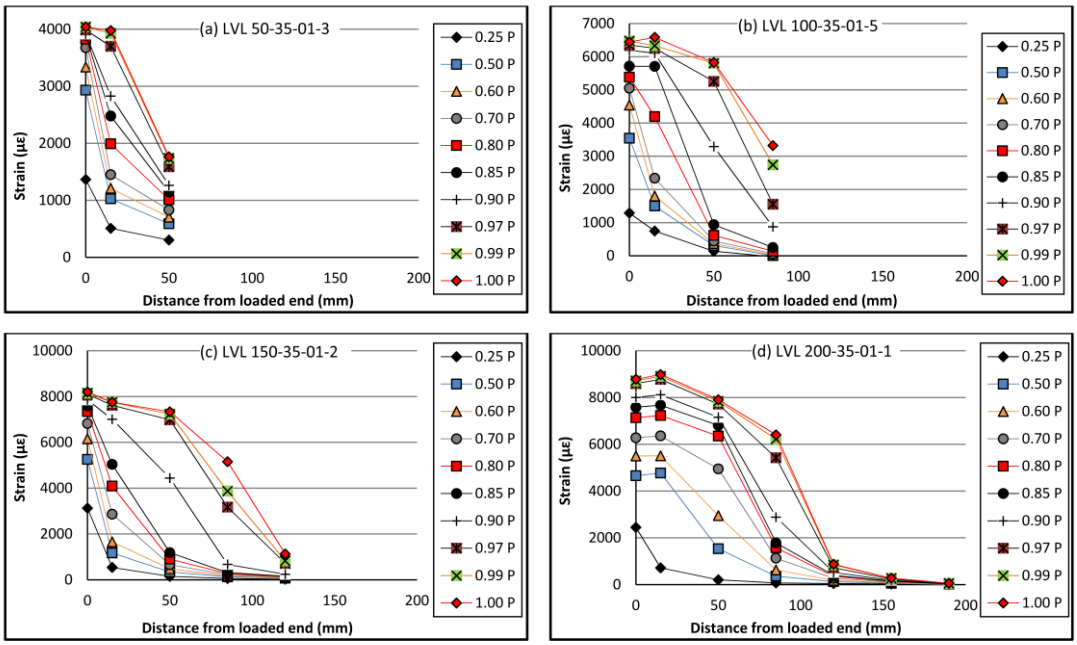

Figure 7, Relationship between strain distribution and bond length

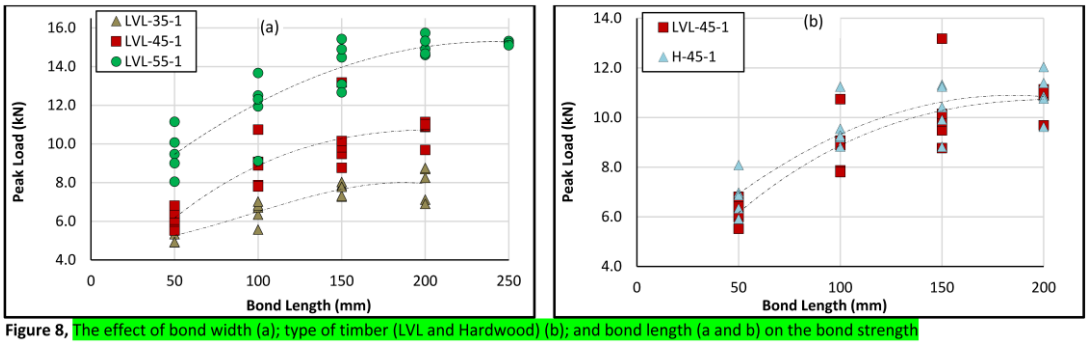

Figure 8, The effect of bond width (a); type of timber (LVL and Hardwood) (b); and bond length (a and b) on the bond strength

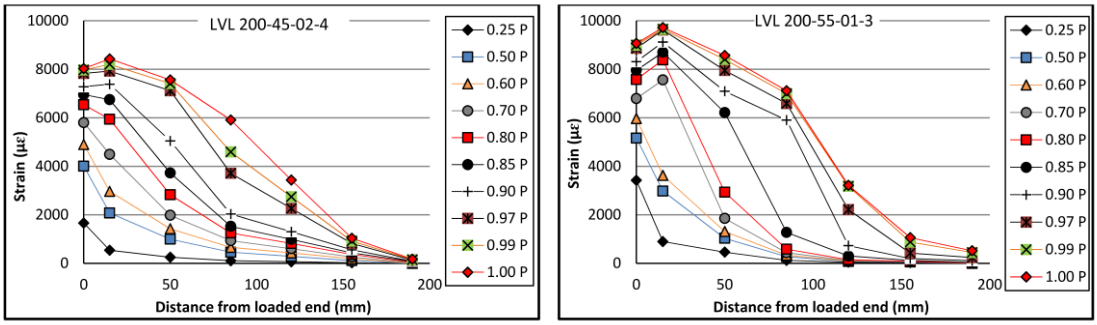

Figure 9, Strain distribution diagrams at various level of applied load

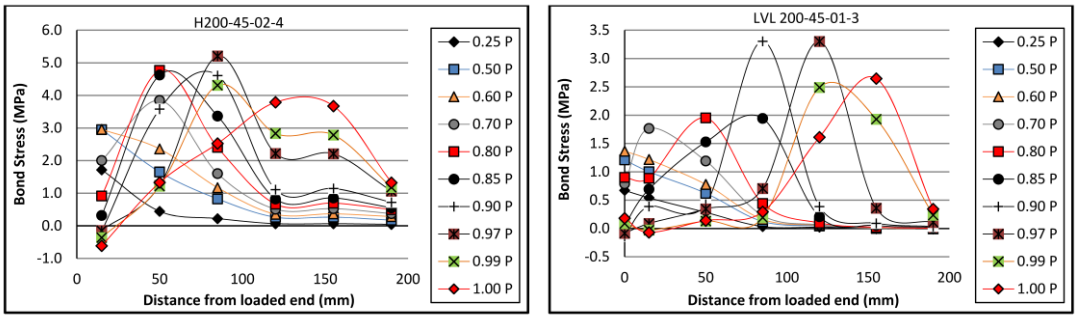

Figure 10, Relationship between bond stress and distance from the loaded end

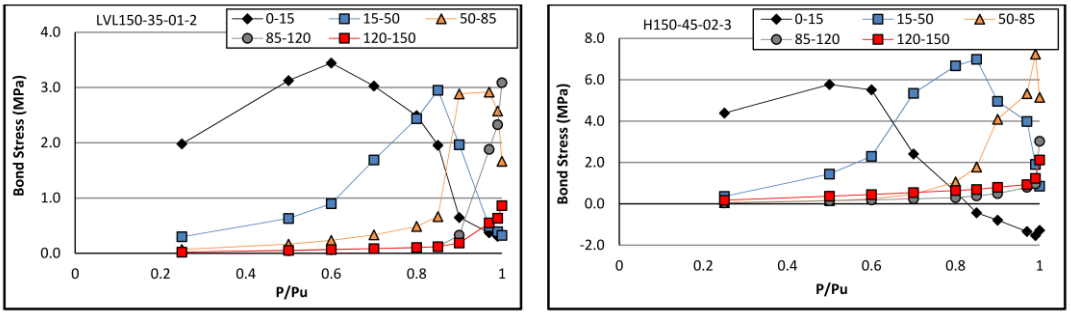

Figure 11 Shear stress as function of relative load level for selected specimens

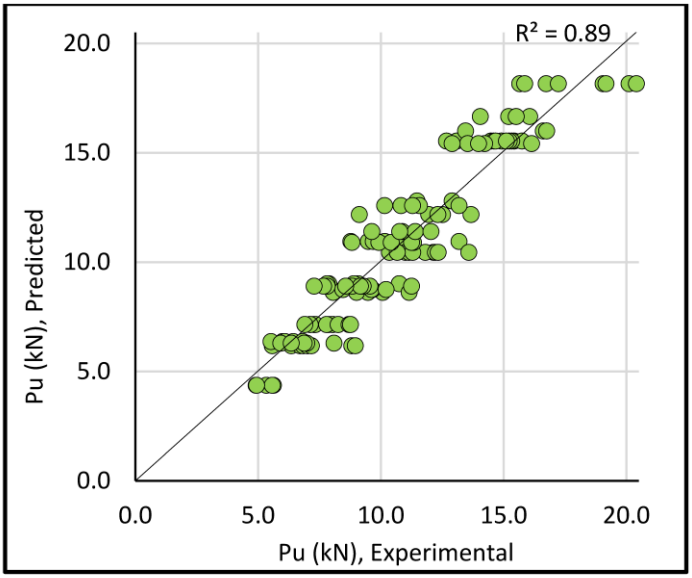

Figure 12, Comparison of predicted bond strength against experimental results

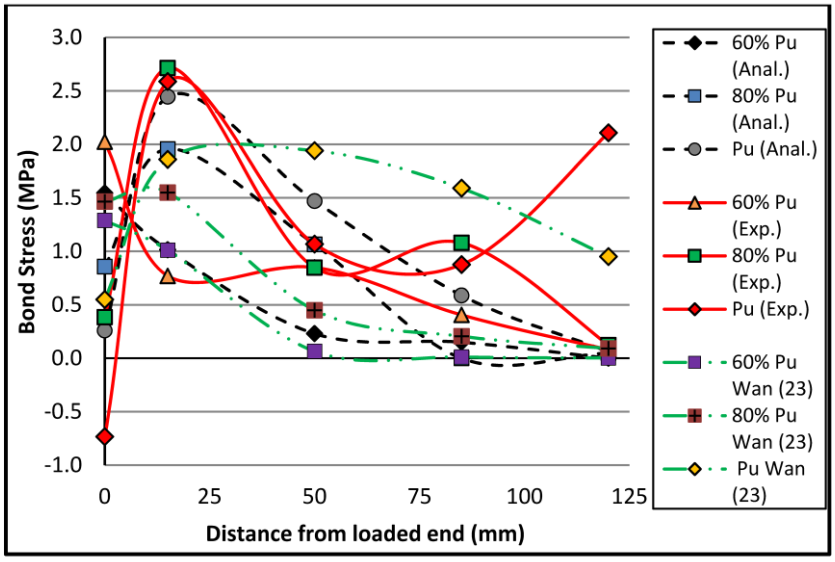

Figure 13, Comparison of shear stress profile against experimental, current analytical model and the model proposed by Wan [23]; H150-45-01-1